

Supporting Information

Importance of spin-triplet excited-state character on the reverse intersystem crossing process of the spiro-based TADF emitters

Jiaqi Li, Tian Tian, Dongxue, Guo, Tingyu Li, Mingfan Zhang, and Houyu Zhang*

State key laboratory of supramolecular structure and materials,

Institute of theoretical chemistry, College of Chemistry, Jilin university,

Changchun 130012, P.R. China

*Email: hoyuzhang@jlu.edu.cn

Contents

Table S1. Calculated HOMO energies of molecule **1** with different DFT functionals.

Table S2. Calculated absorption and emission wavelengths of molecule **1** with different functionals.

Table S3. Calculated dihedral angles and the changes between any two different states for the investigated molecules.

Table S4. Calculated HOMO and LUMO levels of the donor and acceptor fragments.

Table S5. Calculated related energies about the reorganization energies for the RISC process.

Table S6. Calculated ratio of population in T₁ and T₂ states.

Table S7. Calculated emission oscillator strength of S₁ states ($f(S_1)$), emission energy of T₁ states ($\Delta E_{em}(T_1)$, eV), the transition energy difference between the S₁→S₀ and T₁→S₀ transitions ($\Delta E(S_1 - T_1)$, eV), and SOC constant ($\langle T_1 | H_{SOC} | S_1 \rangle$, cm⁻¹) for the investigated molecules.

Fig. S1 Schematic diagram of the potential energy surfaces and computational details about TADF.

Fig. S2 Optimized geometrical structures of the investigated molecules.

Fig. S3 FMO plots of the orbitals involved in the exciton transitions for the investigated molecules.

Fig. S4 NTO analysis for S₁, T₁, and T₂ states of the investigated molecules.

Table S1. Calculated HOMO energies of molecule **1** with different DFT functionals with a fixed percentage of nonlocal Hartree-Fock exchange (HF_{exc}).

HF_{exc}	B3LYP 20%	PBE0 25%	BMK 42%	CAM-B3LYP 19% at SR and 65% at LR	Exptl. ^a
HOMO (eV)	-5.18	-5.42	-5.87	-6.47	-5.53

^aExptl: from ref. 47.

Table S2. Calculated absorption wavelength (λ_{abs}) of molecule **1** in dichloromethane solution and the emission wavelength (λ_{em}) in toluene solution with different DFT functionals with a fixed percentage of nonlocal Hartree-Fock exchange (HF_{exc}).

HF_{exc}	B3LYP 20%	PBE0 25%	BMK 42%	CAM-B3LYP 19% at SR and 65% at LR	Exptl. ^a
λ_{abs} (nm)	535	496	406	351	400
	368	350	312	295	320
λ_{em} (nm)	682	622	496	411	520

^aExptl: from ref. 47.

Table S3. Calculated dihedral angles (α as indicated in Fig. 2, in degree) in the ground and excited states and the changes of twisted angles between any two different states ($\Delta\alpha$) for the investigated molecules.

	S₀	S₁	T₁	 S₁-S₀ 	 T₁-S₀ 	 T₁-S₁
1	66.5	65.9	68.5	0.6	2.0	2.6
2	66.2	66.7	67.6	0.5	1.4	0.9
3	87.2	85.3	83.9	1.9	3.3	1.4
4	85.3	89.8	89.9	4.5	4.6	0.1
5	67.4	68.6	67.5	1.2	0.1	1.1
6	88.7	84.8	87.1	3.9	1.6	2.3

Table S4. Calculated HOMO and LUMO levels of the donor fragments **1d** and **2d**, and acceptor units **1a**, **2a**, and **3a** at the PBE0/6-31G(d, p) level.

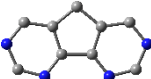
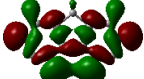
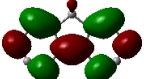
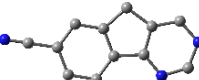

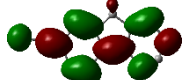
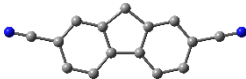
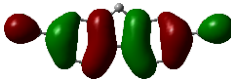
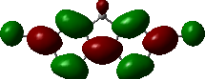
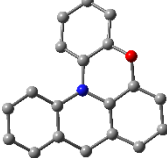
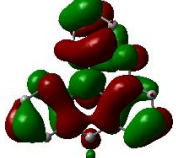
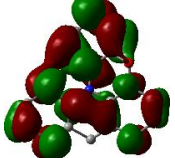
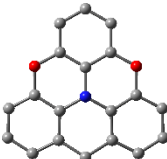
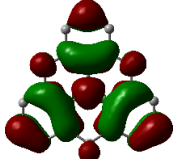
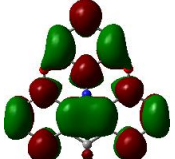
	Structure	HOMO		LUMO	
1a			-7.36 eV		-2.14 eV
2a			-7.31 eV		-2.19 eV
3a			-7.00 eV		-2.27 eV
1d			-5.04 eV		-0.33 eV
2d			-4.82 eV		-0.49 eV

Table S5. Calculated related energies about the reorganization energies for the RISC process.

	E_s (S_1 -geometry)	E_s (T_1 -geometry)	λ (hartree)	λ (eV)
1	-1506.19537546	-1506.18608110	0.00929436	0.253
2	-1446.07948599	-1446.07924422	0.00024177	0.007
3	-1580.20418594	-1580.20399119	0.00019475	0.005
4	-1520.08811430	-1520.08794455	0.00016975	0.004
5	-1385.95612932	-1385.95586249	0.00026683	0.008
6	-1459.96528452	-1459.95057405	0.01471047	0.400

Table S6. Calculated ratio of population in T_1 and T_2 states.

Mol.	1	2	3	4	5	6	2S	5S
$T_2:T_1$	71:1	26:1	126:1	8:1	101:1	3:1	53:1	20:1

Table S7. Calculated emission oscillator strength of S₁ states ($f(S_1)$), emission energy of T₁ states ($\Delta E_{em}(T_1)$, eV), the transition energy difference between the S₁→S₀ and T₁→S₀ transitions ($\Delta E(S_1 - T_1)$, eV), and SOC constant ($\langle T_1 | H_{SOC} | S_1 \rangle$, cm⁻¹) for the investigated molecules.

Mol.	$f(S_1)$	$\Delta E_{em}(T_1)$	$\Delta E_{em}(T_1)^3$	$\Delta E(S_1-T_1)$	$\langle T_1 H_{SOC} S_1 \rangle$
2	0.0004	2.516	15.927	0.015	0.012
2S	0.0005	2.536	16.310	0.026	0.080
5	0.0007	2.558	16.738	0.018	0.015
5S	0.0008	2.526	16.118	0.106	0.165

Comments on the k_p for molecules **2, **2S**, **5**, and **5S**:**

For molecules **2**, **2S**, **5**, and **5S**, the introduction of sulfur atom will lead to the increase of SOC which is favorable to increasing k_p . However, the calculated k_p for **5S** is lower than **5**. Since the k_p depends not only on the SOC, but also the $f(S_n)$, $E(T_1)$, and $\Delta E(S_n-T_1)$. We can understand this from k_p expression from the T₁ state to the S₀ state as follows:

$$k_p^\alpha(T_1 \rightarrow S_0) = \frac{16 \times 10^6 \pi^3 \eta^3 E(T_1)^3}{3 \epsilon_0 h} \left[\sum_n \frac{\langle T_1^\alpha | H_{SOC} | S_n \rangle}{\Delta E(S_n - T_1)} \right] \mu(S_n)$$

The relevant physical quantities (Table S7) are closely related to the k_p values for the emissive triplet state T₁, such as $f(S_n)$, $E(T_1)$, $\Delta E(S_n-T_1)$, and $\langle T_1 | H_{SOC} | S_n \rangle$. The values of $f(S_n)$, $\Delta E(S_n-T_1)$ and $\langle T_1 | H_{SOC} | S_n \rangle$ become larger with the introduction of sulfur atom, which are different from the value of $\Delta E_{em}(T_1)$. Although molecule **5** has a small SOC constant, the small $\Delta E(S_n-T_1)$ value, large $\Delta E_{em}(T_1)$, and similar $f(S_1)$ are beneficial to gain a large k_p . On the contrary, a small $\Delta E_{em}(T_1)$ of **5S** lead to a lower k_p in comparison to **5**. Thus, the $\Delta E_{em}(T_1)$ is the main influencing factor of molecule **5S**.

Fig. S1 Schematic diagram of the potential energy surfaces and computational details about TADF.



Fig. S2 Structural changes between the optimized structures of S₀ and S₁, S₀ and T₁, and S₁ and T₁ states (S₀, S₁, and T₁ structures are depicted in grey, red, and blue, respectively). Root mean square displacement ($\text{RMSD} = \sqrt{\frac{1}{N} \sum_i^{\text{atom}} [(x_i - x'_i)^2 + (y_i - y'_i)^2 + (z_i - z'_i)^2]}$) between S₁ and T₁ states.

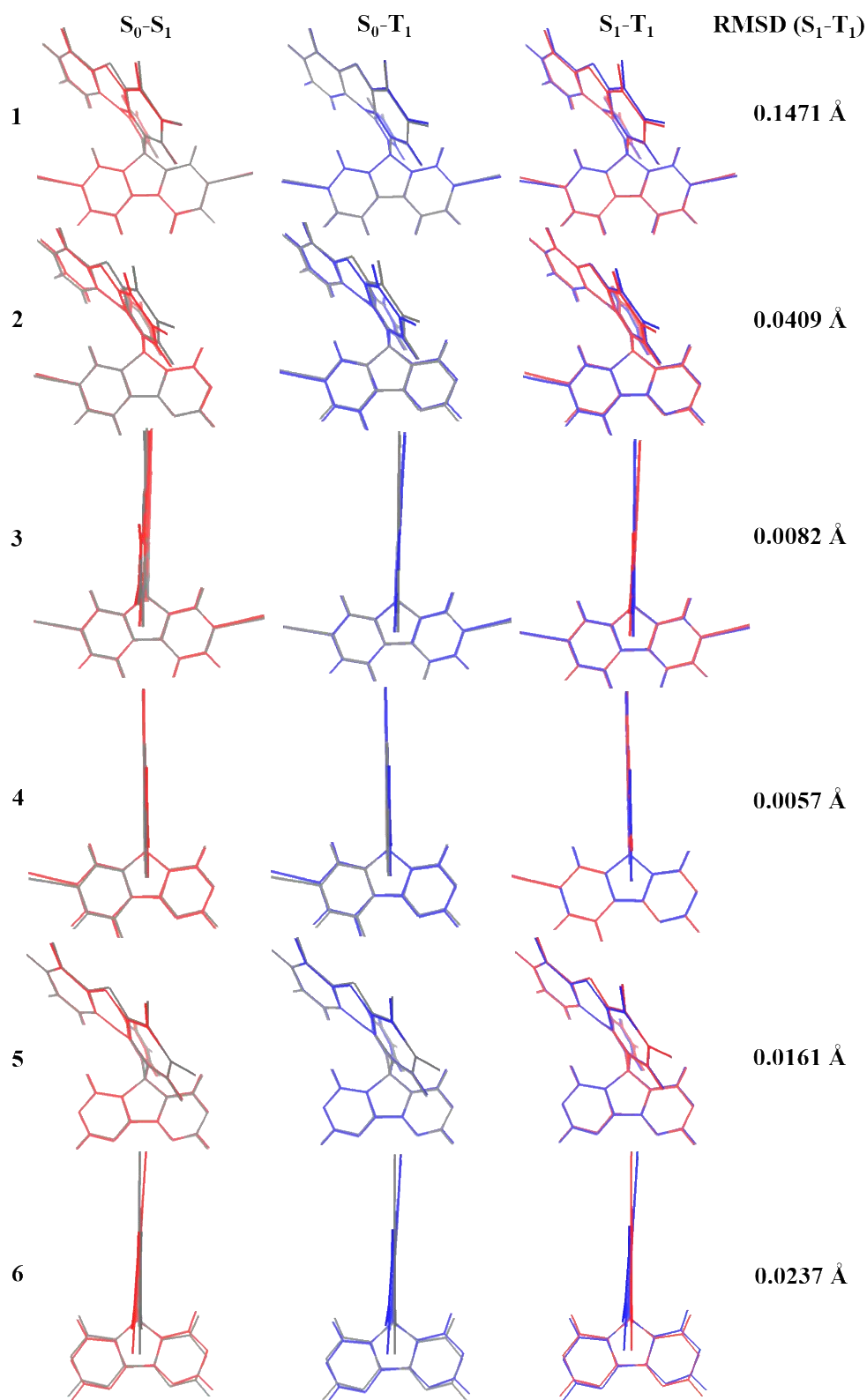


Fig. S3 FMO plots of the orbitals involved in the exciton transitions for the investigated molecules.

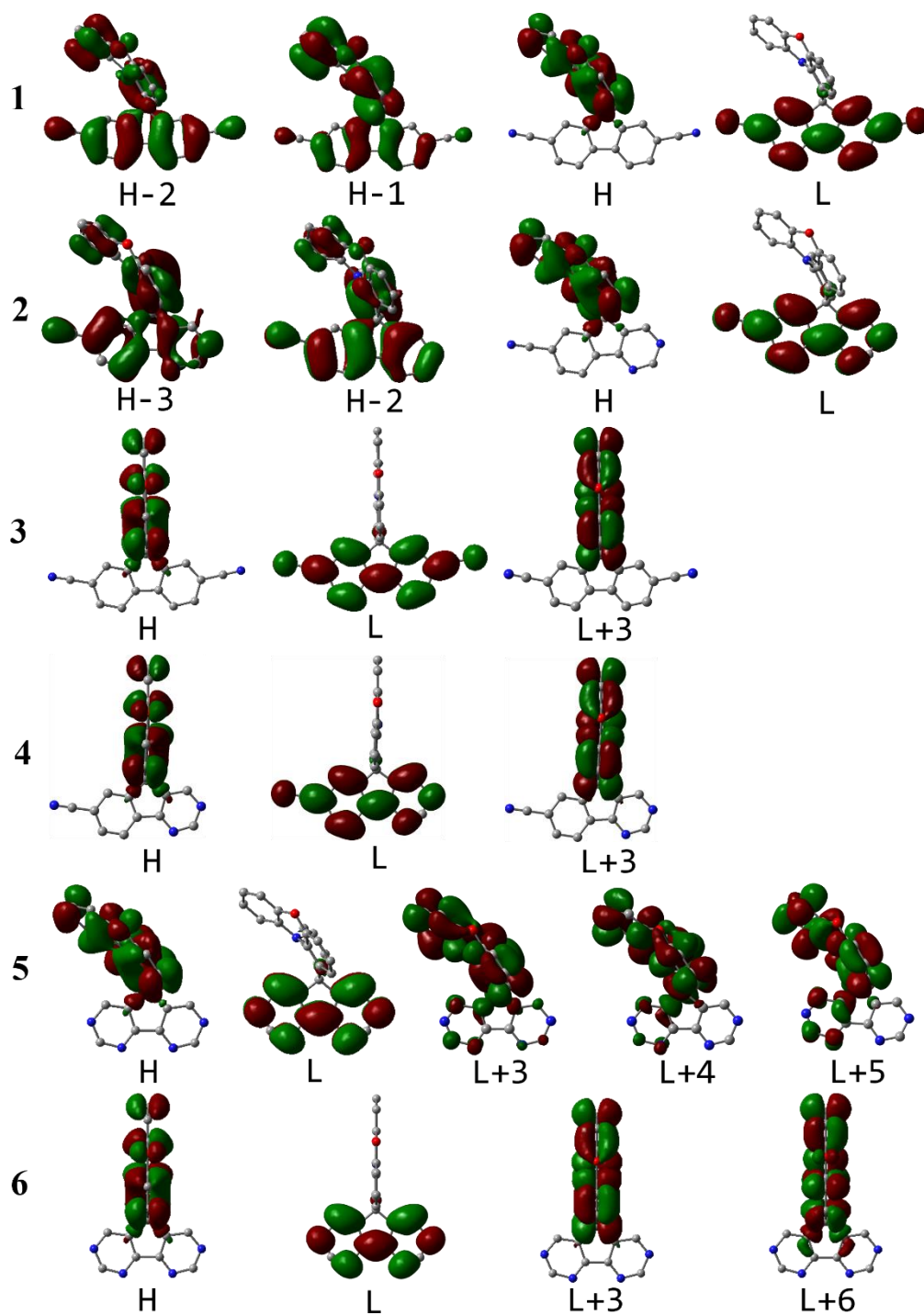


Fig. S4 NTO analysis for S_1 , T_1 , and T_2 states of the investigated molecules.

